

# Speed Control of Photovoltaic Pumping System

Hamza Bouzeria<sup>\*‡</sup>, Cherif Fetha<sup>\*</sup>, Tahar Bahi<sup>\*\*</sup>, Salima Lekhchine<sup>\*\*</sup>, Lotfi Rachedi<sup>\*</sup>

<sup>\*</sup>Department of Electrical Engineering, Laboratory (LEB), Hadj Lakhdar University, 05000, Batna, Algeria

<sup>\*\*</sup>Department of Electrical Engineering, Badji Mokhtar University, 23000, Annaba, Algeria

(bhamza23000@gmail.com, cheriffetha@gmail.com, tbahi@hotmail.com, slekhchine@yahoo.fr, nouflot@yahoo.fr)

<sup>‡</sup>Corresponding Author; Hamza Bouzeria, Department of Electrical Engineering, Laboratory (LEB), Hadj Lakhdar University, 05000, Batna, Algeria, Tel: +213 771 247 853, bhamza23000@gmail.com

*Received: 21.07.2014 Accepted: 29.08.2014*

**Abstract-** In this paper, an intelligent speed controller of permanent magnet synchronous motor is investigated. The motor speed leads a photovoltaic water pumping system. The photovoltaic generator is connected to chopper converter that is controlled by technical fuzzy logic with a view to operate can be tracked the maximum power point whatever the temperature and solar irradiance variation. Thus, to analyze the performance of speed control between the proportional integrator controller and fuzzy logic controlled. A synthesis of these speed controllers is developed and the simulations with Matlab/Simulink according to the progressive and abrupt load tests are shown and discussed.

**Keywords** Photovoltaic, water pumping, fuzzy logic controller, MPPT, simulation.

## 1. Introduction

Due to the ever increasing demand in power, several laboratories have oriented their research design and the development of structures for the production of electrical energy [1-3].

In particular, the geographical location of the Algeria that is strategic with the average solar daily amount on the horizontal plane is in order of 5 to 7 kWh/m<sup>2</sup>/day and an average daily sun is of the order of 7 to 9 hours [4]. However, the decision maker's aim through the encouragement of the production of electrical energy based solar energy in order to solve the problem of managing energy for isolated areas.

The PV system has the disadvantage of a low efficiency, low performances and a very high cost. Furthermore, the photovoltaic generator (PVG) is non-linear, including its operation or the maximum power (MPP) which depend of irradiation, temperature and a variation of a load [5, 6].

Therefore, monitoring of the maximum power point tracking (MPPT) used as a strategy to control DC - DC converter online to track the maximum output power point for PVG to various climatic conditions of operation. The reference of DC voltage is obtained by the MPPT algorithm [7]. There are many methods for calculating the MPPT [8-12]. Among which is the most used is the perturbation and

observation method, other techniques have been developed equally offered, in order, with the hope of minimizing the number of devices or enhance performance of generating the control signal Pulse Width Modulation (PWM) of DC-DC converters .

In this work, we consider the study of a photovoltaic pumping system. This system plays the role of an essential means to need water for remotes areas. Although it accepts big quantities of solar radiation throughout the year, so PV water pumping system (PVWPS) is perfectly solution of water in sahara sites [13].

There is provided this system for controlling the speed of a permanent magnet motor synchronous (PMSM) which is supplied a centrifugal pump. The PMSM is primarily used because of their relatively low cost and robustness [14]. Where, this motor was supplied by power AC converter. The role of the fuzzy observer is designed to optimize the overall performance of the system, leading accordingly to maximize the speed and flow of water from the centrifugal pump coupled with the speed of rotation and modular variable number of work steps to obtain the highest system performance for all conditions [15].

The continuation of this article is made up of the following sections: Section II discusses the modelling system topologies of photovoltaic water pumping systems and

features. Section III deals the space vector pulse modulation. Section IV discusses the MPPT based on fuzzy logic. Section IV discusses the speed control of PMSM based on fuzzy logic controller (FLC) and compare with traditional PI regulator. Finally, Section V presents the simulation and results obtained with the proposed techniques.

## 2. Modelling of System

The structure of photovoltaic water pumping considered in this work is illustrated by “Fig. 1”.

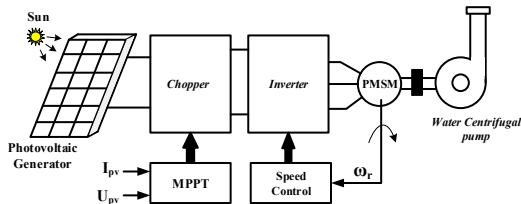


Fig. 1. Synoptic bloc of photovoltaic water pumping

### 2.1. Photovoltaic Generator

A cell photovoltaic is component the most elementary of a module PV [16], the current generated by these cells is very weak. A solar module is a combination amongst solar cells, which are joined in series  $N_s$  or shunt  $N_p$  in order to increase the power of a PV module, it's modelled as a power current ( $I_{ph}$ ) with diode ( $D$ ) in parallel, shunt and series resistance designed respectively by  $R_{sh}$  and  $R_s$ . The model circuit of PV array is indicated in “Fig. 2”.

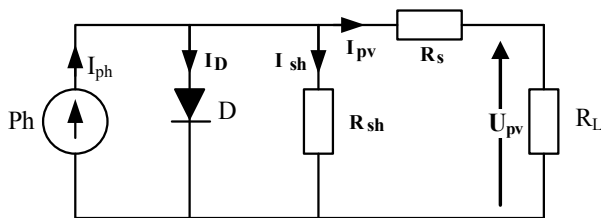


Fig. 2. Equivalent circuit for the photovoltaic model

The main electrical equation of PV module is illustrated by “Eq. (1)” [17, 18]:

$$I_L = I_{ph} - I_D - I_{sh} \quad (1)$$

$$I_L = N_p I_{ph} - N_p I_0 \left\{ \exp \left[ \frac{q(U_{pv} + I_L R_s)}{akT N_s} \right] - 1 \right\} - \frac{U_{pv} + I_L R_s}{R_{sh}} \quad (2)$$

Where,

$I_L$ : output load current;

$U_{pv}$ : output voltage of PV array;

$I_{ph}$ : photocurrent of cell solar;

$R_{sh}$ ,  $R_s$ : shunt and series resistance, respectively;

$q$ : electron quantity's  $= 1,60217646 \times 10^{-19}C$ ;

$k$ : boltzmann's constant.  $k=1,3806503 \times 10^{-23}J/K$ ;

$a$ : ideal factor of the PV characteristic  $1 < a < 1,5$ ;

$I_0$ : current of saturation reverse cell is given by following

Equation:

$$I_0 = I_{or} \left( \frac{T}{T_r} \right)^3 \exp \left\{ \frac{qE_G}{ka} \left[ \frac{1}{T_r} - \frac{1}{T} \right] \right\} \quad (3)$$

With,

$$I_{or} = \frac{I_{scn}}{\left( \frac{qV_{ocn}}{a.N_s.k.T_r} \right) - 1} \quad (4)$$

Where,

$T$ ,  $T_r$ : real and reference temperature, respectively;

$I_{or}$ : saturation reverses current;

$E_G$ : energy band gap of semiconductor;

$V_{ocn}$ : nominal open-circuit voltage of the PV module.

Indeed, the relation of photocurrent ( $I_{ph}$ ) is represented by the following relation:

$$I_{ph} = \{ I_{scr} + k_i(T - 298) \} \frac{G}{1000} \quad (5)$$

Where,

$I_{sc}$ : short-circuit current;

$G$ : solar radiation;

$k_i$ : coefficient of short-circuit current temperature.

The previous equations show that the climatic conditions radiation solar ( $G$ ) and temperature ( $T$ ) have a considerable impact on the amplitude of the voltage and current of PVG. “Fig. 3” and “Fig. 4” show the variation of power and current depending on the voltage for solar radiation between 200  $W/m^2$  to 1000  $W/m^2$  at constant temperature ( $T=25^\circ C$ ) and the deferent temperature for  $-5^\circ C$  to  $55^\circ C$  with constant solar radiation ( $G=1000 W/m^2$ ), respectively.

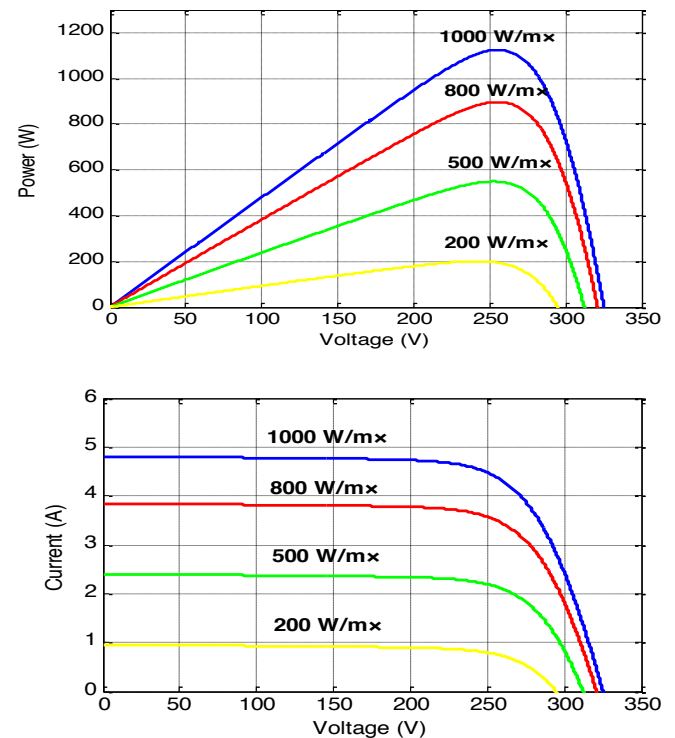
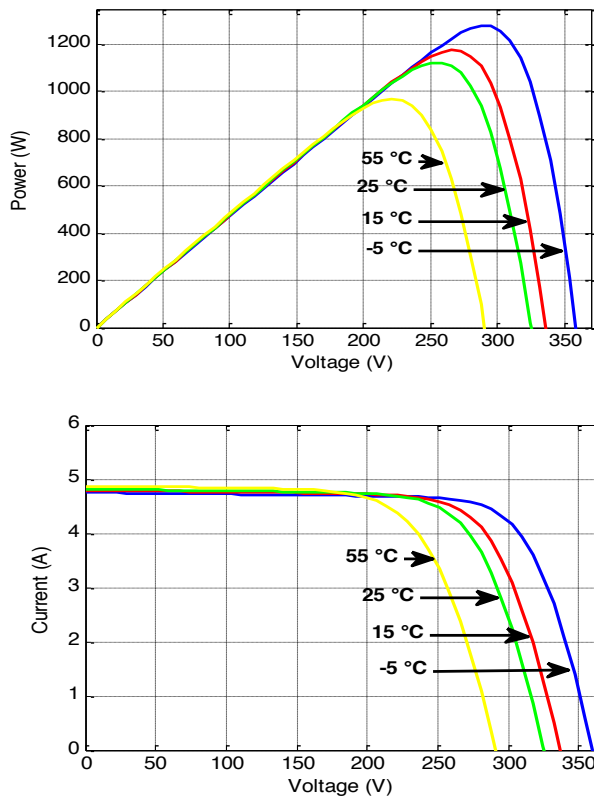


Fig. 3. Power and current characteristics for different solar radiation



**Fig. 4.** Power and current characteristics for different temperature

**2.2. Chopper Model**

The power supplied by the photovoltaic generator feeds the boost converter, it is used as a voltage regulator. This regulation is used the Pulse Width Modulation (PWM) strategy where the switching devices (MOSFETs, IGBTs) are controlled by MPPT based on fuzzy logic controller. The MPPT controller required the optimum duty cycle of the semiconductor, who depends of atmospheric conditions, is shown in “Fig. 5”.

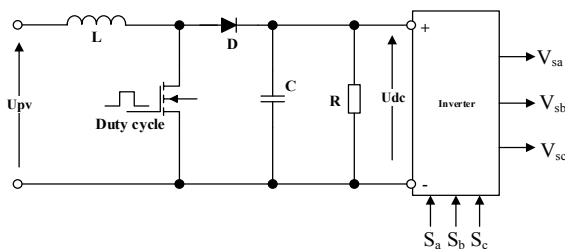


**Fig. 5.** DC-DC converter circuit schema

The relations “Eq. (6)” can express the output voltage of the boost converter [19, 20].

$$U_{dc} = \frac{U_{pv}}{1-D} \tag{6}$$

**2.3. PWM Inverter Model**

The three-phase inverter is inserted between the chopper and the AC motor is composed of three independent arms, each arm possesses two semiconductors controlled by the Space Vector Pulse Width Modulation (SVPWM) [21]. The

stator voltages of PMSM ( $V_{sa}, V_{sb}, V_{sc}$ ) and the photovoltaic current ( $I_{pv}$ ) with  $S_a, S_b$  and  $S_c$  are the pulses generator applied for semiconductors which are exposed respectively as following:

$$\begin{bmatrix} V_{sa} \\ V_{sb} \\ V_{sc} \end{bmatrix} = \frac{U_{pv}}{3} \begin{bmatrix} 2 & -1 & -1 \\ -1 & 2 & -1 \\ -1 & -1 & 2 \end{bmatrix} \begin{bmatrix} S_a \\ S_b \\ S_c \end{bmatrix} \tag{7}$$

$$I_{pv} = S_a i_{sa} + S_b i_{sb} + S_c i_{sc} + I_c \tag{8}$$

Where,  $i_{sa}, i_{sb}$  and  $i_{sc}$  are the PMSM stator currents and

$$I_c = c \frac{dU_{pv}}{dt}$$

**2.4. Permanent Magnet Synchronous Motor Model**

PMSM model in alpha-beta axis reference can be described by the following mathematical equations:

$$\begin{cases} u_\alpha = R_{st} i_\alpha + \frac{L_{st} di_\alpha}{dt} - \omega_r \Psi_f \sin \theta \\ u_\beta = R_{st} i_\beta + \frac{L_{st} di_\beta}{dt} - \omega_r \Psi_f \cos \theta \end{cases} \tag{9}$$

$$\begin{cases} \Psi_\alpha = \int (u_\alpha - R_{st} i_\alpha) dt \\ \Psi_\beta = \int (u_\beta - R_{st} i_\beta) dt \end{cases} \tag{10}$$

$$T_e = \frac{3}{2} N_p (\Psi_\alpha i_\beta - \Psi_\beta i_\alpha) \tag{11}$$

Where,

$u_\alpha, u_\beta$ : stator voltage component of PMSM;

$i_\alpha, i_\beta$ : stator current components of PMSM;

$R_{st}, L_{st}$ : the stator resistance and the inductance, respectively;

$\Psi_f$ : flux of permanent magnet;

$\omega_r, \theta$ : rotor speed and position, respectively.

**2.5. Centrifugal Pump Model**

The square of the centrifugal pump torque is proportional to the motor rotation speed motor. Centrifugal pump is the most commonly employed type of pumps, it's capable of pumping the water with high volumes due to its efficiency and its top relatively [22, 23]. The performances ( $Q, H$  and  $P$ ) are given in terms of the speed using the following relationships:

$$\begin{cases} Q' = Q \cdot Z \\ H' = H \cdot Z^2 \\ P' = P \cdot Z^3 \end{cases} \tag{12}$$

With  $Z = \omega' / \omega$ ;

where,

$\omega', \omega$ : speed and nominal speed, respectively;

$Q', Q$ : water flow and the nominal water flow, respectively;

$H', H$ : height and total height, respectively;

$P', P$ : power and nominal power, respectively.

**3. Space Vector Pulse Width Modulation**

The SVPWM technique of reducing torque ripples, current and keep a form of circular flow. Therefore, the

SVPWM control delivers a modulator separated for each of the three phases, and then the vector of control overall approximated over a period gives reference voltages. Firstly, SVPWM is made to generate impulses at switches inverter that powers the PMSM motor using the effective voltage vector.

This technique is much in demand in the field of the control, it's effect on ripple current and torque are remarkable, which is why it is the most used by researchers and industry, it is used to determine the sequence of ignitions and extinctions components of the converter and thus to minimize the harmonics and obtain optimum performance of the applied machine voltages. SVPWM technique is different from that at PWM place to employ a separate each phase modulator, the reference voltages are given by a vector approximated overall control over modulation. Especially since the recent technological advances in field of digital computers (DSP, microprocessors and microcontrollers), made his industrial location pretty simple.

The structure of two levels of three phase inverter allows generate eight (08) the vectors voltages which are presented according "Fig. 6". Particularly, two vectors (V0=000 and V7=111) are zero, this to defined the six sectors.

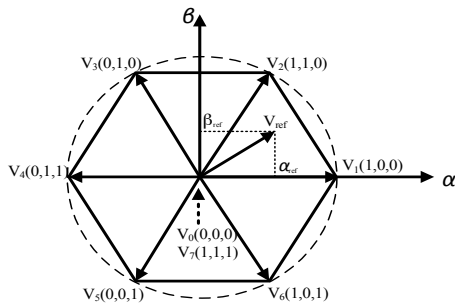


Fig. 6. Voltages space vector diagram for the two-level inverter

3.1. Judgment of Sector Number

The judgement of sector is defined according to the following variables:

$$\begin{cases} U_{ref a} = U_{\beta} \\ U_{ref b} = U_{\alpha}\sqrt{3} - U_{\beta} \\ U_{ref c} = -U_{\alpha}\sqrt{3} - U_{\beta} \end{cases} \quad (13)$$

"Equation (14)" gives the section number (N) [23]. The "Table 1" shows the corresponding relation between N and sector:

$$N = \text{Sign}(U_{ref a}) + 2 \cdot \text{Sign}(U_{ref b}) + 4 \cdot \text{Sign}(U_{ref c}) \quad (14)$$

Where Sign (U<sub>refi</sub> (with i=a, b and c)) is the Sign function.

According to the reference vectors, we obtained the switching states are shown in the following table:

Table 1. Relationship of N and sector number

|               |   |   |   |   |   |   |
|---------------|---|---|---|---|---|---|
| N             | 3 | 1 | 5 | 4 | 6 | 2 |
| Sector number | 1 | 2 | 3 | 4 | 5 | 6 |

3.2. Calculation of Switch Time

From the vectors for different sectors, table 2 shows the execution time of each switch of the inverter,

Table 2. T<sub>1</sub> and T<sub>2</sub> in different sectors

|               |    |   |    |    |    |    |
|---------------|----|---|----|----|----|----|
| Sector number | 1  | 2 | 3  | 4  | 5  | 6  |
| T1            | -Z | Y | X  | Z  | -Y | -X |
| T2            | X  | Z | -Y | -X | -Z | Y  |

With,

$$\begin{cases} X = U_{\beta} \cdot T\sqrt{3}/U_{dc} \\ Y = (3U_{\alpha} + U_{\beta}\sqrt{3})T/2U_{dc} \\ Z = (-3U_{\alpha} + U_{\beta}\sqrt{3})T/2U_{dc} \end{cases} \quad (15)$$

3.3. Definition Time Value of Voltage Vector

The vector voltage time is given according to the following sector:

$$\begin{cases} S_a = (T - T_1 - T_2)/4 \\ S_b = 0,5T_1 + S_a \\ S_c = 0,5T_2 + S_b \end{cases} \quad (16)$$

Assign T<sub>1cs</sub>, T<sub>2cs</sub> and T<sub>3cs</sub> according to "Table 3", where the action time of three phase are defined and compared with triangular wave, finally we obtained deferent time of SVPWM.

Table 3. Time of sector point T<sub>CSP</sub>

|               |                |                |                |                |                |                |
|---------------|----------------|----------------|----------------|----------------|----------------|----------------|
| Sector number | 1              | 2              | 3              | 4              | 5              | 6              |
| T1cs          | S <sub>b</sub> | S <sub>a</sub> | S <sub>a</sub> | S <sub>c</sub> | S <sub>c</sub> | S <sub>b</sub> |
| T2cs          | S <sub>a</sub> | S <sub>c</sub> | S <sub>b</sub> | S <sub>b</sub> | S <sub>a</sub> | S <sub>c</sub> |
| T3cs          | S <sub>c</sub> | S <sub>b</sub> | S <sub>c</sub> | S <sub>a</sub> | S <sub>b</sub> | S <sub>a</sub> |

4. Fuzzy Logic for MPPT Controller

The controller which is based on fuzzy logic is called artificial intelligence, it's becoming increasingly popular where used for tracking the MPPT. It is possess the advantage of this technique is that it can operate with low precision values of input and does not require modelling of the system and processes the linear and nonlinear operation. The principle of fuzzy logic is based on two input variables: the error and the derivative of the error, it is also based on an output variable which is called the duty cycle; it is the trigger converter to wait for the maximum power point that waits it is determined by a rule table. In the blurred literature, it involves three steps: fuzzification, inference and defuzzification. The "Fig. 7" presents the diagram of fuzzy logic.

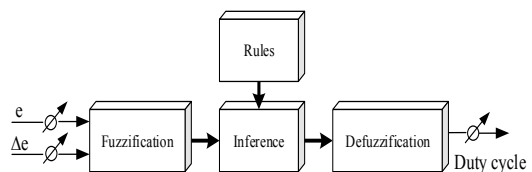


Fig. 7. Structure of fuzzy logic controller

The input parameters are associated with the following equations [24]:

$$\begin{cases} e(k) = \frac{P_{pv}(k) - P_{pv}(k-1)}{V_{pv}(k) - V_{pv}(k-1)} \\ \Delta e(k) = e(k) - e(k-1) \end{cases} \quad (17)$$

Where,

$P_{pv}(k)$ : instantaneous power of PVG,  $V_{pv}(k)$ : instantaneous voltage of PVG.

The fuzzy logic tracks the MPP using the rule of “If A and B, Then C” [24, 25] and the inference calculates the output of the fuzzy logic. Those several methods for inference among the best methods known is Mamdani. And other types for example: compositional rule of inference (CRI), Generalized Modus Ponens (GMP) and Sugeno inference method. In our work the defuzzification applied the center of gravity method to specific the optimum value of duty cycle (d) of FLC [24, 26]:

$$d = \frac{\sum_{i=1}^n (d_i) \cdot \mu(D_i)}{\sum_{i=1}^n \mu(D_i)} \quad (18)$$

In the fuzzification stage, variable digital inputs are converted into linguistic variable in our case with the seven values NB: Negative big; NM: Negative medium NS: Negative small; Z: Zero; PS: Positive small; PM: Positive medium; PB: Positive big, as seen in “Fig. 8”.

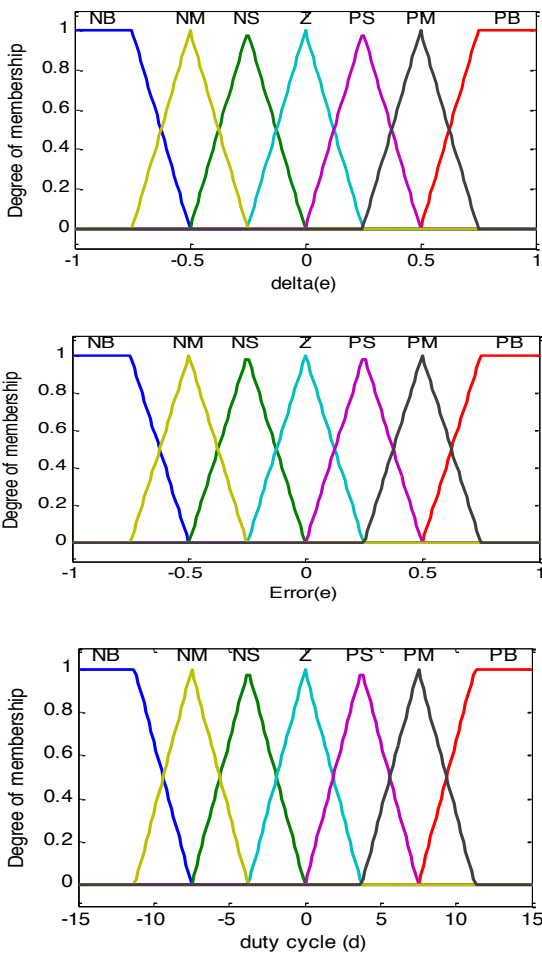


Fig. 8. Rules of fuzzy logic controller

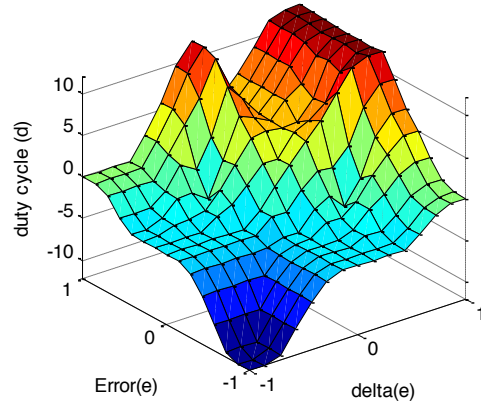


Fig. 9. Surface of fuzzy logic controller

The inference rules will be illustrated in “Table 4” with two input variables as (e) and ( $\Delta e$ ) where (d) as the output.

Table 4. Fuzzy rules

| $\Delta e$   e | NB | NM | NS | Z  | PS | PM | PB |
|----------------|----|----|----|----|----|----|----|
| NB             | NB | NM | NS | NS | NS | NS | Z  |
| NM             | NM | NM | NS | NS | NS | Z  | Z  |
| NS             | NS | NS | NS | NS | Z  | NS | PM |
| Z              | NS | NS | NS | Z  | PS | PM | PM |
| PS             | NS | NS | Z  | PS | PS | PS | PS |
| PM             | NS | Z  | NS | PM | PS | PM | PM |
| PB             | Z  | PS | PM | PB | PB | PB | PB |

### 5. Speed Controller

As shown in equation (12), the beginning of photovoltaic pumping water according to the speed rotation of the PMSM motor which drives the centrifugal pump, then we must add a speed controller returns to the start of water constant.

In our work we concenter two types of controllers: a classic controller is the proportional integral (PI) and fuzzy logic (FLC).

#### 5.1. Proportional Integral Regulator

The traditional regulator PI is the most used in regulation because it is simple and reliable in operation. So in our case we used the PI for speed control of PMSM, so the rotor speed ( $\omega_r$ ) and compared with the reference speed ( $\omega_{ref}$ ). As shown in the following equations [27]:

$$\begin{cases} er(x) = \omega_r(x) - \omega_r(x-1) \\ \Delta er(x) = er(x) - er(x-1) \end{cases} \quad (19)$$

The quadrate current reference is given by:

$$I_{q,ref}(x) = I_{q,ref}(x-1) + K_p \cdot \Delta er(x) + K_i \cdot er(x) \quad (20)$$

Where,

$er(x)$ : speed error of working interval,

$er(x-1)$ : speed error of previous interval,

$K_p$  and  $K_i$ : proportional and integrator speed controller gains, respectively.

5.2. Fuzzy Logic Controller

The fuzzy controller is an intelligent controller defines the laws of control of all the system from adopting rules, he composed two inputs: error and variation in the error rate as expressed in equation (21):

$$\begin{cases} er(x) = \omega_r(x) - \omega_r(x - 1) \\ \Delta er(x) = er(x) - er(x - 1) \end{cases} \quad (21)$$

The “Fig. 10” presents the speed control system then we concede in our paper.

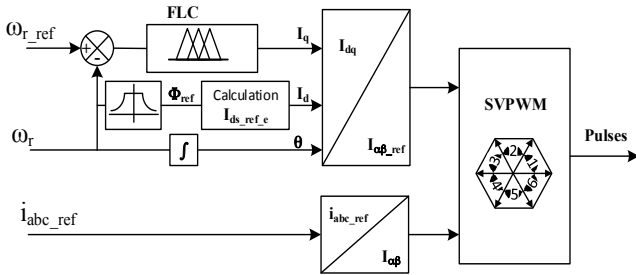


Fig. 10. Speed control of PMSM

6. Speed Controller

The simulation results of the PV water pumping system are presented. “Fig. 11” presents the simulation diagram of considered system.

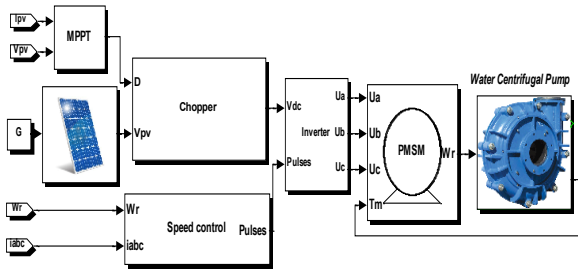


Fig. 11. Simulation block

“Fig. 12” indicates the evolution of the output voltage, power and current of the photovoltaic generator. We note that the fuzzy controller gives better efficiency in response time of about 0.04s and exceeded acceptable.

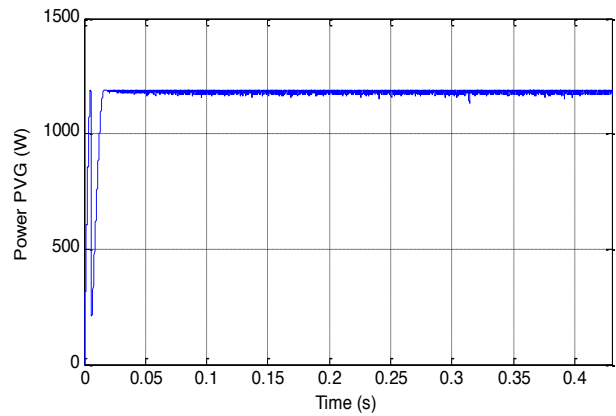
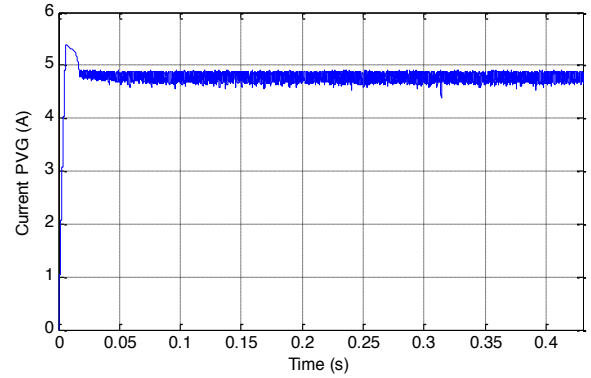
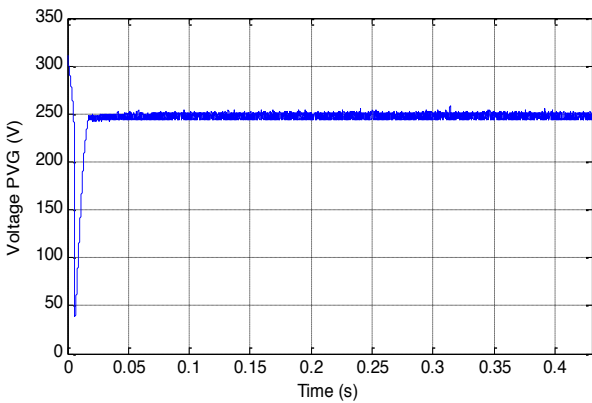
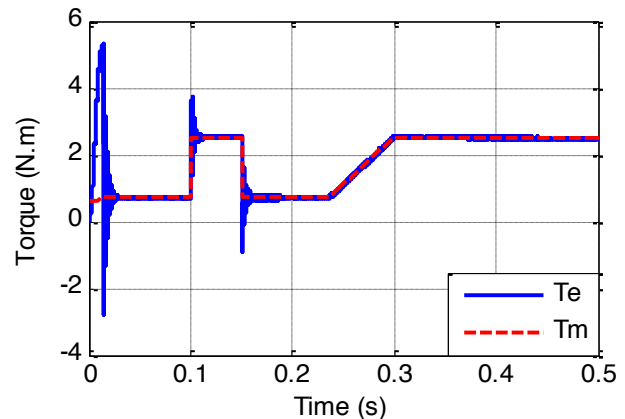
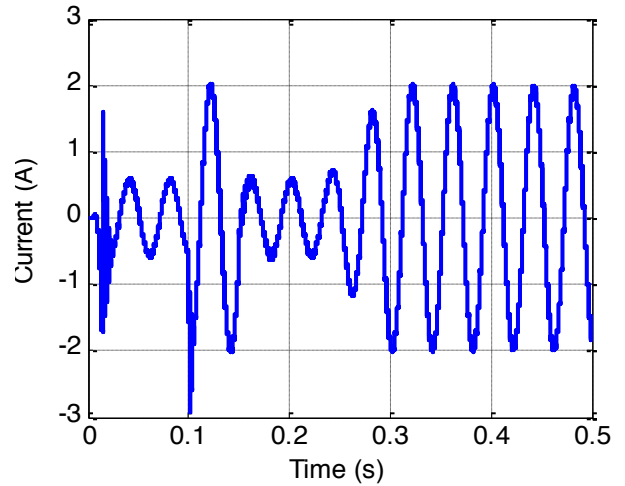
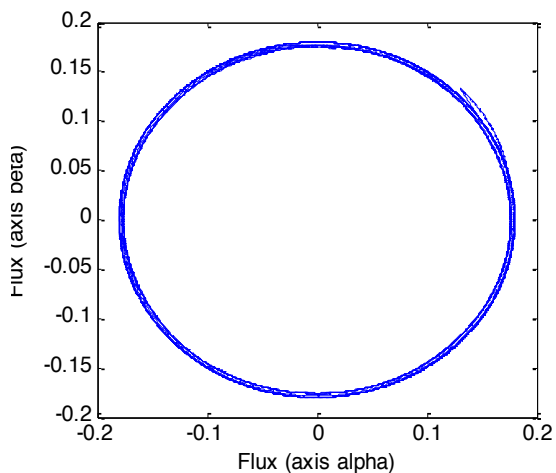


Fig. 12. Voltage, current and power of PVG





**Fig. 13.** Response of current, electromagnetic and flux controlled by FLC

Depending on the nature of the variation of the load, both tests are introduced. Abruptly changes the mechanical torque ( $T_m$ ) of 1N.m to 3.5N.m at time 0.1s to 0.15s, and progressive change of  $T_m$  between 0.25s and 0.3s.

The “Fig. 13” and “Fig. 14” show the test results of control for photovoltaic pumping speed based on FLC and compared with PI corrector. These results show that the fuzzy control ensures the best performances and the oscillations decrease during the starting and the change of the load. Regarding the “Fig. 15” we can see any disturbance of the speed during the progressive load variation.

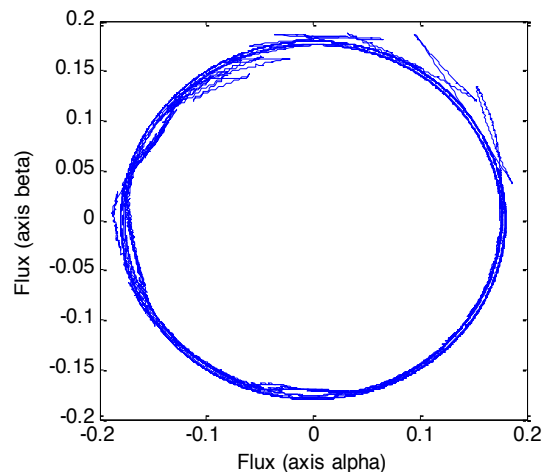
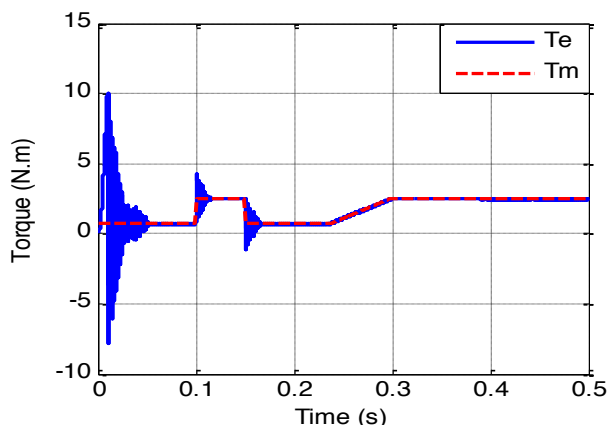
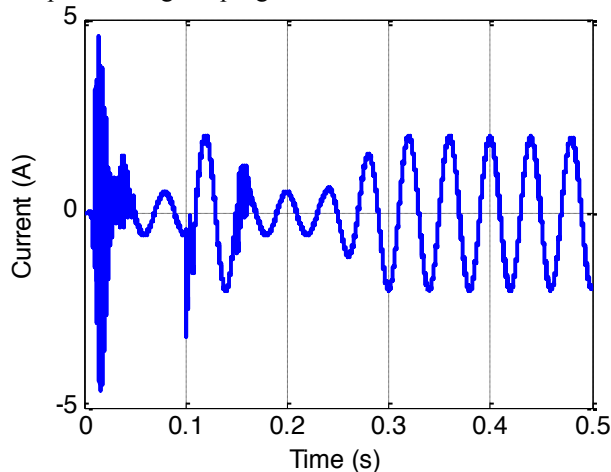


**Fig. 14.** Response of currents, electromagnetic and flux controlled by PI

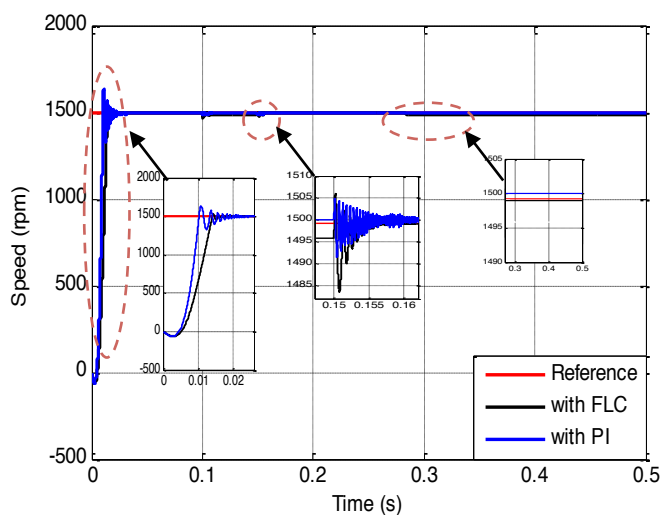


**Fig. 15.** Speed control of PMSM.

## 7. Conclusion

The objective of this paper is to study the tracking current and voltage of solar array for to get the optimum point power maximum possible of the PVG. In other, to get regardless of the different climatic conditions such as solar radiation and temperature.

The artificial intelligence controllers can give more performance than traditional controllers for non-linear systems order, since it's most fast, stable and more flexibility was obtained.

The presented method the water quantity regulation based for PMSM which is supplied by photovoltaic system. The speed is controlled by fuzzy controller.

The comparison of the tests results indicates the acceptability of fuzzy logic controller efficiencies. On balance, it made dynamic conditions state. Indeed, there was a greater speed, a good rejection of load disturbance.

## Appendix

Table 5. System Parameters

| PVG Parameters                            |                 |
|---|-----------------|
| Ppv = 84,62 (Wc)                          | Upv = 17,2 (v)  |
| Ipv= 4,85(A)                              | Ns=15 and Np=1  |
| PMSM parameters                           |                 |
| Rs=2.875( $\Omega$ ),                     | Ls=Lr=0.175 (H) |
| J=0.08 (Kg.m <sup>2</sup> ) and P=4 pairs | N=1470 (tr/min) |
| Centrifugal pump parameters               |                 |
| Q = 2 (l/s)                               | H=10 (m)        |

## References

- [1] J. Clerk Maxwell, A Treatise on Electricity and Magnetism, 3rd ed., vol. 2. Oxford: Clarendon Press, 1892, pp.68-73. (Book)
- [2] P. Bajpai, V. Dash, "Hybrid renewable energy systems for power generation in standalone applications", Renewable and Sustainable Energy Reviews, Vol. 16, No. 5, pp. 2926-2939. June 2012.
- [3] R. Kumar, M. A. Rosen, "A critical review of photovoltaic-thermal solar collectors for air heating", Applied Energy, Vol. 88, N<sup>o</sup>. 11, pp 3603-3614, November 2011.
- [4] C. Lin, C. Huang, D. Yi-Chun, J. Chen, "Maximum photovoltaic power tracking for the PV array using the fractional-order incremental conductance method", Applied Energy, Vol. 88, No. 12, pp 4840-4847, December 2011.
- [5] L. Shuhui, A.H. Timothy, L. Dawen, H. Fei, "Integrating photovoltaic and power converter characteristics for energy extraction study of solar PV systems", Renewable Energy, Vol. 36, No. 12, pp. 3238-3245, December 2011.
- [6] K. June-Min, K. Bong-Hwan, N. Kwang-Hee, "Grid-connected photovoltaic multistring PCS with PV current variation reduction control", IEEE Transactions on Industrial Electronics, Vol. 56, No. 11, pp. 4381-4388, December 2008.
- [7] A. Chaouachi, R.M. Kamel, K. Nagasaka, "A novel multi-model neuro-fuzzy-based MPPT for three-phase grid-connected photovoltaic system", Solar Energy, Vol. 84, No. 12, pp. 2219-2229, December 2010.
- [8] Y. Himri, AS. Malik, A. Boudghene Stambouli, S. Himri, B. Draoui, "Review and use of the Algerian renewable energy for sustainable development", Renewable and Sustain Energy Reviews, Vol. 13, Issues. 6-7, pp 1584-1591, August-September 2009.
- [9] KH. Hussein, I. Muta, T. Hoshino, M. Osakada, "Maximum photovoltaic power tracking an algorithm for rapidly changing atmospheric conditions". IEE Proceedings-Generation, Transmission and Distribution; Vol. 142, No. 1, DOI:10.1049/ip-gtd:19951577, pp. 59-64. January 1995.
- [10] T. Noguchi, S. Togashi, R. Nakamoto, "Short current pulse based maximum power point tracking method for multiple photovoltaic and converter module system", IEEE Trans Ind Electron 2002; Vol. 49, No. 1, pp .217-223, February 2002.
- [11] N. Fernia, G. Petrone, G. Spagnuolo, M. Vitelli, "Optimization of perturb and observe maximum power point tracking method". IEEE Trans Power Electron, Vol. 20, No. 4, pp.963-973, July 2005.
- [12] C. Dorofte, U. Borup, F. Blaabjerg, "A combined two method MPPT control scheme for grid-connected photovoltaic systems". Int Proc Eur Conf Power Electron Appl, pp. 1-10, DOI:10.1109/EPE.2005.219714, September 11-14, 2005.
- [13] T. Esram, J.W. Kimball, P.T. Krein, P.L. Chapman, P. Midya, "Dynamic maximum power point tracking of photovoltaic arrays using ripple correlation control", IEEE Trans Power Electron, Vol. 21, No. 5, pp. 1282 - 1291, September 2006.
- [14] M.P. Alberto, A. Jorge, J.P. Miguel, A.M. Juan, "A modular strategy for isolated photovoltaic systems based on microcontroller", Renewable Energy, Vol. 34, No. 7, pp. 1825-1832, July 2009.
- [15] F.F.M. El-Sousy, "Hybrid-Based Wavelet-Neural-Network Tracking Control for Permanent-Magnet Synchronous Motor Servo Drives", IEEE Trans. Ind. Electron, vol. 57, no. 9, pp. 3157-3166, September. 2010.
- [16] H. Chaoui, P. Sicard, "Adaptive Fuzzy Logic Control of Permanent Magnet Synchronous Machines With Nonlinear Friction", IEEE Transactions on Industrial Electronics, DOI: 10.1109/TIE.2011.2148678, Vol. 59, No. 2, February 2012.
- [17] T. Salmi, M. Bouzguenda, Adel Gastli, A. Masmoudi, "Matlab/Simulink Based Modelling of Solar Photovoltaic Cell", International Journal of Renewable Energy Research, Vol. 2, No. 2, 20 February 2012.
- [18] M. Dris, B. Djilani, "Comparative Study of Algorithms (MPPT) Applied to Photovoltaic Systems", International Journal of Renewable Energy Research, Vol.3, No.4, 14 November 2013.
- [19] Y.S. Kumar, R. Gupta, "Maximum power point tracking of multiple photovoltaic arrays", Students Conference on Engineering and Systems (SCES), DOI: 10.1109/SCES.2012.6199027, March 2012.
- [20] C. Ben Salah, M. Ouali, "Comparison of fuzzy logic and neural network in maximum power point tracker

- for PV systems” ,Electric Power Systems Research, Vol.81, pp. 43-50, January 2011.
- [21] A. Kalirasu,S. SekarDash, “Simulation of Closed Loop Controlled Boost Converter for Solar Installation” Serbian Journal of Electrical Engineering, Vol.7,pp.121-130, May 2010.
- [22] Dr. Adel, A. Elbaset, Dr.B.M. Hasaneen, “Design and simulation of DC/DC boost converter” ,The Twelfth International Middle East Power System Conference, Egypt, vol. 1 ,March 2008.
- [23] S.G. Malla, C.N. Bhende, S. Mishra, “Photovoltaic based Water Pumping System”, International Conference on Energy, Automation and Signal (ICEAS), 28-30,India, December2011.
- [24] X. Wang, Y. Xing, Z. He, Y. Liu, “Research and Simulation of DTC Based on SVPWM of PMSM”, Procedia Engineering, International Workshop on Information and Electronics Engineering, DOI: 10.1016/j.proeng.2012.01.195,Vol. 29, pp. 1685–1689, 2012.
- [25] A. Panda, M.K. Pathak, S.P. Srivastava, “Solar Direct Torque Controlled Induction Motor Drive for Industrial Applications”, International Journal of Renewable Energy Research, Vol. 3, No. 4, December, 2013.
- [26] M.S. AïtCheikh, C. Larbes, G.F. TchoketchKebir, A. Zerguerras,“Maximum power point tracking using a fuzzy logic control scheme”, Renewable Energy, Vol.10, No. 3, pp.387–395, 2007.
- [27] Y. Wu, B. Zhang, J. Lu, K.L. Du, “FuzzyLogic and Neuro-Fuzzy System A Systemetic Introduction”, International Journal of Artificial Intelligence and Expert Systems,Vol. 2, No. 2, pp 47-80, 2011.
- [28] A. Terki, A. Moussi, A. Betka, N. Terki, “An improved efficiency of fuzzy logic control of PMBLDC for PV pumping system”, Applied Mathematical Modelling, Vol. 36, No. 3, DOI : 10.1016/j.apm.2011.07.042, pp. 934–944, March 2012.